Communications to the Editor

Crystallization in the Presence of a Liquid−Liquid Phase Separation

Stéphane Veesler,* Eve Revalor, Olivier Bottini, and Christian Hoff[†]

Centre de Recherche en Matière Condensée et Nanosciences, CRMCN-CNRS Campus de Luminy, Case 913, F-13288 Marseille Cedex 9, France

Abstract:
This paper presents and compares crystallization experiments of an active pharmaceutical ingredient and a biological molecule in the presence of a liquid−liquid phase separation monitored by in situ video. The advantage of this setup is that it requires a small quantity of these products to study the influence of the physicochemical parameters on crystallization. Crystallization mechanisms and kinetics are different depending on the starting position in the phase diagram and on the temperature reduction, when crystallization is temperature-induced. Liquid−liquid phase separation changes the medium and the conditions of crystallization, hinders both primary and secondary nucleation for several hours, and consequently affects the process. For great temperature reduction and, inside the spinodal zone, namely high supersaturation (> 15), crystals nucleate inside the droplets. Therefore, we take advantage of the formation of droplets to propose a new approach to spherical crystallization. The final products are quasi-spherical monodisperse agglomerated particles of about 500 μm made up of small crystals of a few micrometers.

Introduction

Crystallizing complex molecules, such as proteins or active pharmaceutical ingredients (API), leads to problems such as formation of different solid (polymorphism) or liquid (demixion) phases and/or poor nucleation ability. Moreover, due to the use of solvent mixtures, phase diagrams are complex. In this contribution, we present a study of the impact of a liquid−liquid phase separation (LLPS) or demixing on solution nucleation and crystallization and we propose a new approach to spherical crystallization[1,2] taking advantage of the complexity of the phase diagram and the presence of a metastable LLPS. In this paper all the LLPSs are temperature-induced; for a composition-induced phase separation see for example Vivares and Bonnete.[3] This type of phase diagram is often observed in protein systems;[4−8]

however to our knowledge, only five cases are documented for small molecules.[9−14] In the examples treated in this paper, an API and a protein, the LLPS lies inside the metastable zone for crystallization and hinders both primary and secondary nucleation for several hours in agreement with the Ostwald rule of stages.[15] After several hours, at high supercooling, preferential primary nucleation occurs inside the droplets. Nucleation, crystal growth, and agglomeration occur inside the droplet producing quasi-spherical particles. Applied to pharmaceuticals, this method has the advantage of combining crystallization and granulation: such spherical agglomerates have good handling and compression properties.[16] This study shows that fully understanding the phase diagram and completely controlling crystallization parameters (temperature, supersaturation, and solution composition) are invaluable in process development.

Methods

Materials. The organic molecule studied (basic formula: $C_{35}H_{41}Cl_2N_3O_2$) is a Sanofi-Aventis API (Scheme 1). This compound crystallizes into two polymorphs, FI and FII, with platelet and needle crystal habits, respectively.[10] The crystallization occurs in an ethanol/water mixture (54.2/45.8% weight). The solubility of the polymorphs is high in ethanol but very low in water.

The biological molecule studied, the BPTI (bovine pancreatic trypsin inhibitor, 6511 Da, pI = 10.5). is employed as an anticoagulant to reduce blood loss during cardiac surgery and was supplied as a lyophilized powder by Bayer and used as received without further purification. The purity

* To whom correspondence should be addressed. E-mail: veesler@crmcn.univ-mrs.fr.
† Current address: Sanofi-Aventis chimie, F-30390 Aramon, France.

(1) Kawashima Y.; Okumura M.; Takenaka H. *Science* **1982**, *216*, 1127−1128.
(2) Sano A.; Kuriki T.; Kawashima Y.; Takeuchi H.; Niwa T. *Chem. Pharm. Bull.* **1989**, *37*, 2183−2187.
(3) Vivares D.; Bonnete F. *J. Phys. Chem. B* **2004**, *108*, 6498−6507.
(4) Berland, C.; Thurston, G.; Kondo, M.; Broide, M.; Pande, J.; Ogun, O.; Benedek, G. *PNAS* **1992**, *89*, 1214−1218.
(5) Muschol, M., R. F. *J. Chem. Phys.* **1997**, *107*, 1953−1961.
(6) Galkin, O.; Vekilov P. G. *J. Am. Chem. Soc.* **2000**, *122*, 156−163.
(7) Grouazel, S.; Perez, J.; Astier, J.-P.; Bonneté, F.; Veesler, S. *Acta Crystallogr.* **2002**, *D58*, 1560−1563.
(8) Gliko, O.; Neumaier, N.; Pan, W.; Haase, I.; Fischer, M.; Bacher, A.; Weinkauf, S.; Vekilov, P. G. *Journal of American Chemical Society* **2005**, *127*, 3433−3438.
(9) Groen, H.; Roberts, K. J. *J. Phys. Chem. B* **2001**, *105*, 10723−10730.
(10) Lafferrere, L.; Hoff, C.; Veesler, S. *Engineering in Life Science* **2003**, *3*, 127−131.
(11) Bonnett, P. E.; Carpenter, K. J.; Dawson, S.; Davey, R. J. *Chemical Communication* **2003**, 698−699.
(12) Lafferrere, L.; Hoff, C.; Veesler, S. *Crystal Growth & Design* **2004**, *4*, 1175−1180.
(13) Deneau, E.; Steele, G. *Org. Process Res. Dev.* **2005**, *9*, 943−950.
(14) Sheikh, A. Y.; Pal, A. E. *Crystallization in the vicinity of liquid−liquid phase separation boundary*; 16th International Symposium on Industrial Crystallization, 2005, Dresden, Germany.
(15) Ostwald W. *Z. Phys. Chem.* **1897**, *22*, 289−330.
(16) Espitalier, F.; Biscans, B.; Laguerie, C. *Chemical Engineering Journal* **1997**, *68*, 103−114.

Scheme 1. Structure of $C_{35}H_{41}Cl_2N_3O_2$, MW 606.6 g mol^{-1}
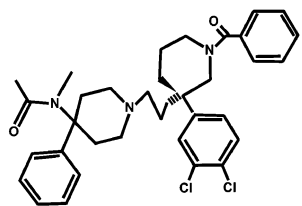
was checked by molecular sieving FPLC.[17] The necessary quantities of BPTI and KSCN were dissolved in pure water (ELGA UHQ reverse osmosis system) to obtain stock solutions for phase separation trials. The different solutions were buffered with acetic acid to 80 mM, adjusted to pH 4.5 with NaOH (1 M), and filtered through 0.22 μm Millipore filters. After dissolution of BPTI, the pH was 4.9. The BPTI concentration was measured by optical density measurements using an extinction coefficient of 0.786 cm^{-1} mL mg^{-1} at 280 nm.[18] In all this study, the salt concentration was fixed at 350 mM KSCN, and the pH, at 4.9.

Phase Diagrams. BPTI solubilties were obtained by seeding supersaturated solutions with small BPTI crystallites. The decrease in protein concentration was charted by spectrophotometry until it remained unchanged for at least 2 weeks. The solubility of both the stable and the metastable polymorphs of $C_{35}H_{41}Cl_2N_3O_2$ versus temperature was determined using the bracketing technique.[19,20] Solutions and crystals were placed in a 2-mL quiescent glass vessel inserted in a thermostated cell under an optical microscope (Nikon Diaphot), and the crystal temperature equilibrium was measured.[21] The same setup was used to observe and to characterize the LLPS for both API and BPTI. The coexistence curve for the liquid phases, also called the T_{L-L} boundary (L—L for liquid—liquid), was determined through light scattering intensity measurements.[7,22]

In addition and solely for the API, LLPS experiments were carried out using a 200 mL batch crystallizer which was a double jacketed glass vessel equipped with four wall baffles to prevent the solution from rotating in the crystallizer. We used a three-blade stainless steel propeller (Mixell TT) to stir at a constant speed of 450 rpm. The crystallizer was rapidly set to different temperatures using a computer-controlled thermostated circulating water bath (Julabo F25). The temperature and turbidity of the solution or the slurry were measured in situ by a platinum resistance thermometer (PT100) and a Mettler-Toledo FSC 402 equipped with OFS12H_407N Mettler-Toledo probe, respectively.

Solid Characterization. Crystals were observed under a scanning electron microscope (SEM) JEOL 6320F. Moreover, all the solid phases were characterized by X-ray diffraction INEL CPS 120.

(17) Veesler, S.; Ferté, N.; Costes, M. S.; Czjzek, M.; Astier, J. P. *Crystal Growth & Design* **2004**, *4*, 1137−1141.
(18) Lafont, S.; Veesler, S.; Astier, J. P.; Boistelle, R. *J. Crystal Growth* **1994**, *143*, 249−255.
(19) Beckmann, W. *Org. Process Res. Dev.* **2000**, *4*, 372−383.
(20) Beckmann, W.; Boistelle, R.; Sato, K. *J. Chem. Eng. Data* **1984**, *29*, 211−214.
(21) Veesler, S.; Lafferrere, L.; Garcia, E.; Hoff, C. *Org. Process Res. Dev.* **2003**, *7*, 983−989.
(22) Lafferrere, L.; Hoff, C.; Veesler, S. *J. Crystal Growth* **2004**, *269*, 550−557.

Results and Discussion

Phase Diagrams. Because in many cases the end products strongly depend on the starting position in the phase diagram, determining the phase diagram is an important step for crystallization studies and process development. Solubilities of $C_{35}H_{41}Cl_2N_3O_2$ and BPTI being high in ethanol and water, respectively, supersaturation is achieved (a) for $C_{35}H_{41}Cl_2N_3O_2$ by antisolvent addition where the poor solvent, water, plays the role of precipitant and (b) for BPTI by salting-out, namely adding KSCN.

The phase diagrams of the API and the protein presented in Figure 1 have previously been determined.[7,22] It clearly appears that the liquid—liquid phase boundary lies below the liquids (solubility curve) for both solutes but inside the metastable zone for crystallization. As a result, the use of a solvent mixture for the sake of the process may lead to a miscibility gap in the phase diagram which affects the crystallization process.

LLPS and Primary Nucleation. The nucleation and growth of droplets of the protein-rich phase in a crystal-free supersaturated solution of BPTI (20 mg/mL, $\beta = C/C_0 = 1.1$ at 22 °C, C and C_0 being the solution concentration and solubility, respectively) are observed in a 2-mL quiescent thermostated crystallizer when the temperature is decreased to 21 °C (Figure 2a−c). When the temperature is increased the dissolution of the droplets is observed (Figure 2d−f). No droplet coalescence is observed. This parallels the finding of other experiments[12] which have shown that when a solution of $C_{35}H_{41}Cl_2N_3O_2$ at a concentration of 14.6% weight in an ethanol/water mixture (54.2/45.8% weight) at 60 °C is cooled to 30 °C ($\beta = 6.8$), droplets appear, grow, and coalesce.

It is noteworthy that no primary nucleation was observed with the protein and the API in the time frame of the experiments for the temperature range tested in this part of the paper, although the solutions were supersaturated with respect to the solid phase. As a result, LLPS (the metastable phase) hinders for several hours solid primary nucleation (the stable phase) in agreement with the Ostwald rule of stages.

LLPS and Secondary Nucleation. Figure 3 shows the nucleation, in a 2-mL quiescent thermostated crystallizer, of droplets in a supersaturated solution of BPTI (24 mg/mL), when the temperature is decreased. The monoclinic crystal present in the micrographs was seeded prior to the LLPS experiment. Note that no nucleation occurred during these experiments with BPTI. Similar seeding experiments have been previously conducted with the API in a stirred crystallizer,[12] and no secondary nucleation was observed.

Despite high supersaturation, $\beta = 2$ for the BPTI and $\beta = 5.8$ and 3.6 for forms I and II of the API, secondary nucleation is hindered. The situation should be completely different for greater temperature reduction as shown in the following section.

LLPS and Spherical Crystallization of the API. We propose that, given the influence of the demixion on crystallization, advantage can be taken of the nucleation of droplets for a new approach to spherical crystallization. Whereas in spherical crystallization[2,23] a quasi-emulsion is
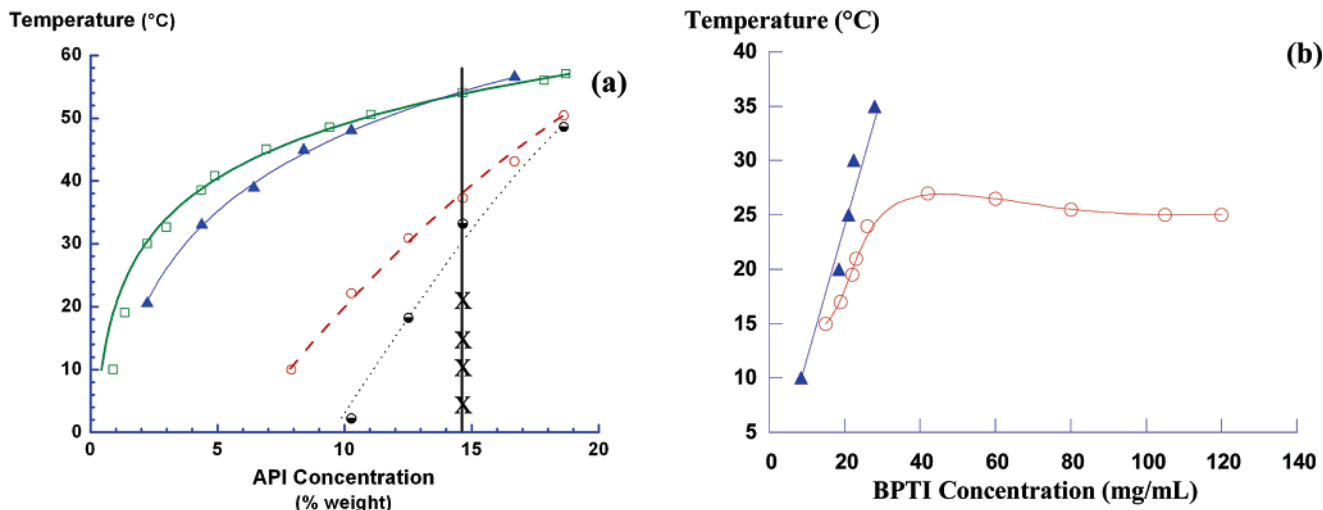
Figure 1. Phase diagrams: (a) of $C_{35}H_{41}Cl_2N_3O_2$ in an ethanol/water mixture (54.2/45.8% weight), with open squares representing solubility of FI, triangles representing solubility of FII, and X corresponding to experiments of section LLPS and Spherical Crystallization of the API, and (b) of BPTI with 350 mM KSCN with triangles representing solubility. Open circles represent cloud point data, and black and white circles, spinodal points. Lines are only guidelines.
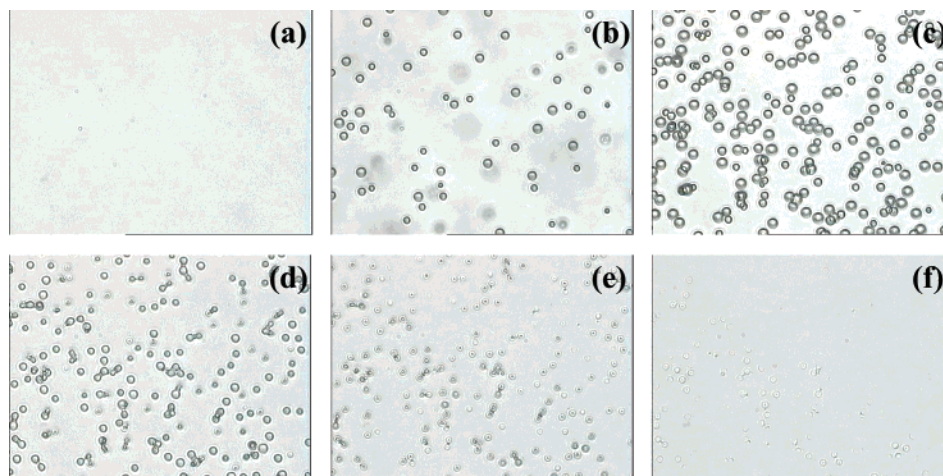
Figure 2. Observation by optical microscopy of the nucleation of droplets of the protein-rich phase in a supersaturated solution of BPTI (20 mg/mL) when the temperature is decreased from 22 to 21 °C (a−c) and dissolution of droplets when the temperature is increased from 21 to 22 °C (d−f). Droplets are about 10 μm.
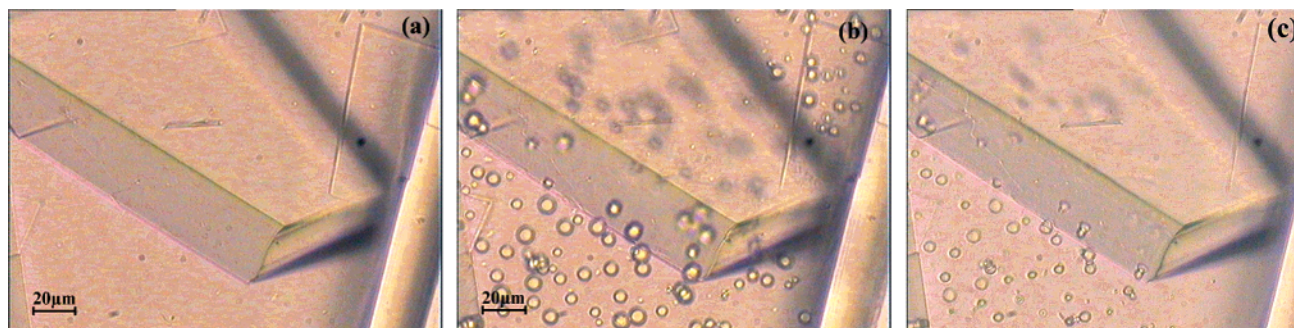
Figure 3. Observation by optical microscopy of the nucleation of droplets of the protein-rich phase in a supersaturated solution of BPTI (24 mg/mL) when the temperature is decreased: (a) $T = 20$ °C ($\beta = 1.4$) and (b) $T = 15$ °C ($\beta = 2$). And dissolution of droplets when the temperature is increased from 15 to 20 °C (c).
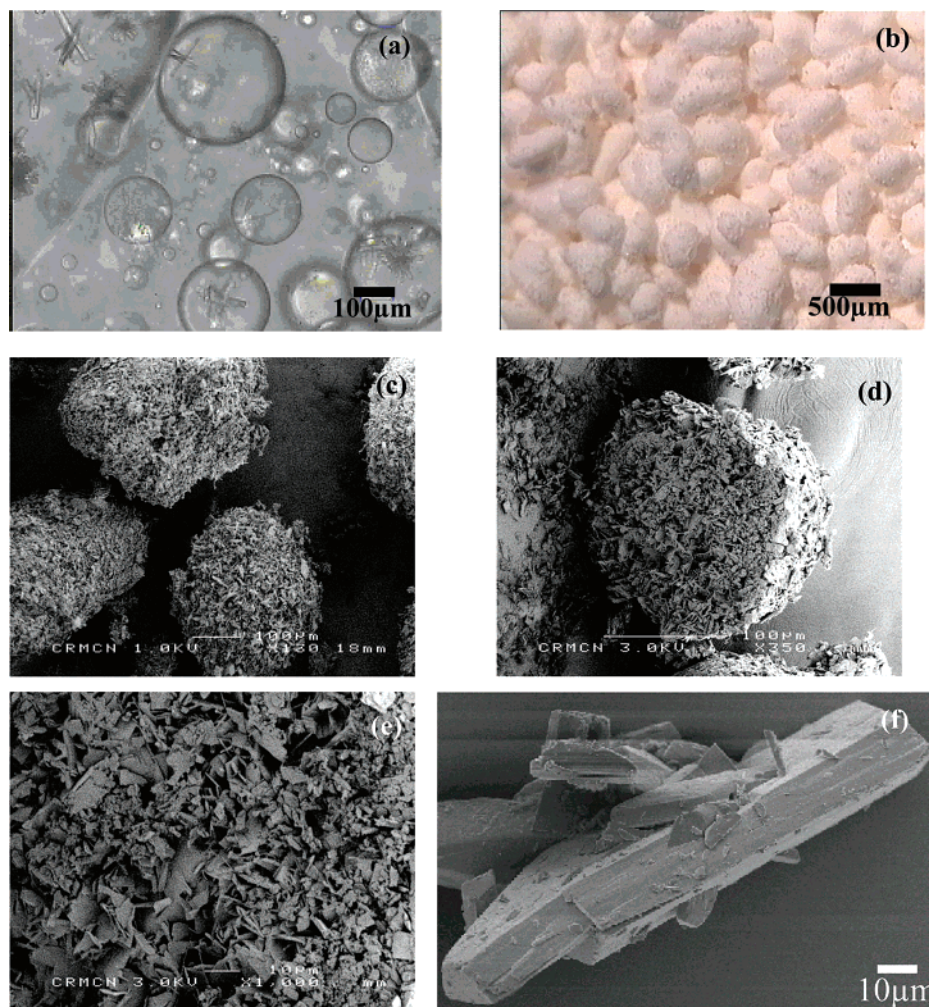
normally formed by addition of a binary mixture of a good solvent and a solute to a poor solvent, we propose to form the quasi-emulsion by temperature variation.

Although LLPS hinders solid primary nucleation (see section LLPS and Primary Nucleation), the situation was

(23) Espitalier, F.; Biscans, B.; Laguerie, C. *Chemical Engineering Journal* **1997**, *68*, 95−102.

completely different for greater temperature reductions producing high supersaturation with respect to the solid phase, $\beta > 15$, i.e., in the spinodal zone for LLPS. To characterize the influence of a greater temperature reduction, different solutions of the API at a concentration of 14.6% weight in an ethanol/water mixture (54.2/45.8% weight) at 60 °C were cooled (X in Figure 1a and Table 1). Experiments

Figure 4. Observation by optical microscopy of the nucleation of crystals in the droplets of the API-rich phase at 20 °C (a) and of particles obtained at the end of the experiment (b), and SEM image of agglomerated crystals of Figure 4b (c), cross sectional view of a particle (d and e) and crystals obtained by classical secondary nucleation and growth experiment [after[10]](f).

Table 1. Experimental conditions (temperature and supersaturation with respect to FI) and approximate size of particles obtained[a]

T (°C)	β	particle size (μm)
20	15.1	450
15	24.0	400
10	32.6	500
5	40.7	500

[a] The size was estimated by optical microscopy.

were performed in a 200 mL crystalliser at a constant stirring rate of 450 rpm; suspensions were withdrawn isothermally and placed in a 2-mL quiescent glass vessel inserted in a thermostated cell under an optical microscope for rapid observation.

In the first stage, $t < 4$ h, droplets appear, grow, and coalesce. In the second stage, from $t > 4$ h to $t = 35$ h, crystals nucleate inside the droplets and grow (Figure 4a). In the last stage, $t > 35$ h, droplets disappear. This stage corresponds to the solution-mediated phase transition of the liquid phase into the solid phase. Finally, after separation by filtration, crystals are observed. The final products are freely flowing quasi-spherical monodispersed agglomerated

particles (Figure 4b) of about 500 μm made up of small crystals of a few micrometers (Figure 4c). A cross section of the particle shows a dense agglomerated structure. Moreover, the crystal habit and size are totally different, compared to crystals obtained by secondary nucleation and growth experiments outside the demixion zone (Figure 4f). In all cases, crystals obtained at the end of the experiment are of FI.

To conclude, although the scale-up of an LLPS is problematic, we demonstrate that by fully understanding the phase diagram, we can transform a disadvantage, namely poor nucleation ability and a demixion, into an advantage, by using crystallization inside the droplets thus producing spherical agglomerates.

Conclusions

In this paper we monitor crystallization experiments of an active pharmaceutical ingredient and a biological molecule by in situ video microscopy to visualize how crystals and droplets change. One of the advantage of this setup is that it requires a small quantity of these products to study the influence of the physicochemical parameters on crystallization.

According to whether the starting position in the phase diagram is inside or outside the liquid−liquid phase separation region, and the degree of temperature reduction, the crystallization mechanisms and kinetics are different. As a consequence, the end products can differ greatly in solid phase, crystal habit, morphology, and size. LLPS changes the medium and the conditions of crystallization, hinders both primary and secondary nucleation for several hours, and consequently affects the process. We take advantage of the nucleation of droplets to propose a new approach to spherical crystallization, when temperature decrease is great (at high supersaturation > 15). We obtain crystals which nucleate inside the droplets, and the final products are quasi-spherical monodispersed agglomerated particles of about 500 μm made up of small crystals of a few micrometers. Future studies should focus on the influence of the hydrodynamics of this process, since particle size is probably related to droplet size.[16]